Journal of Materials Chemistry

www.rsc.org/materials

Volume 20 | Number 29 | 7 August 2010 | Pages 5969–6196

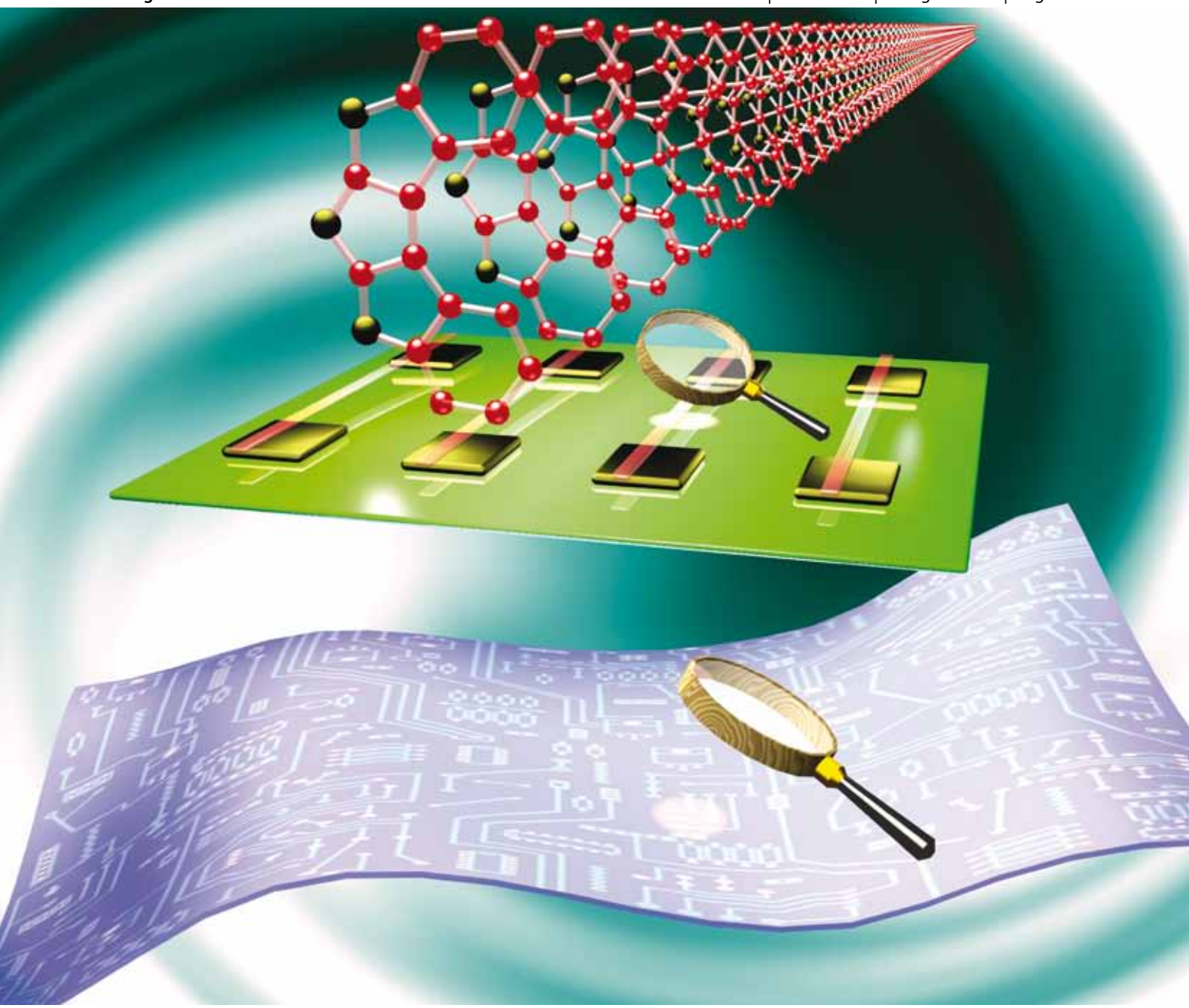

ISSN 0959-9428

RSC Publishing

0959-9428(2010)20:29;1-I

Single crystal ribbons and transistors of a solution processed sickle-like fused-ring thienoacene†

Rongjin Li,[ab] Huanli Dong,[a] Xiaowei Zhan,*[a] Yudong He,[a] Hongxiang Li[b] and Wenping Hu*[a]

Received 7th April 2010, Accepted 27th May 2010
DOI: 10.1039/c0jm00963f

A fused-ring thienoacene with sickle-like molecular shape was synthesized and examined in self-assembly and in transistors for the first time. Different from the linear fused-ring thienoacenes with herringbone packing motif, the sickle-like thienoacene exhibits a π–π molecular packing motif and could self-assemble into one-dimensional single crystalline ribbons efficiently. Moreover, the compound demonstrates not only excellent solubility in common organic solvents, but also high mobility and stability in transistors, indicating the great application prospect of the compound in organic electronics.

Introduction

The fundamental advantages of organic semiconductors have attracted the world's attention recently and resulted in the rapid development of organic electronics.[1] For example, the solution process ability of organic semiconductors not only allows unconventional deposition methods (such as printing) for device fabrication at low cost, but also provides the possibility for efficient self-assembly of structures with desired properties from solution. And the most distinguished feature is that the structural versatility of organic semiconductors allows for the incorporation of functionalities by molecular design. Certainly, there are still open challenges for further advancement of organic electronics such as the low mobility and stability of most organic semiconductors and the lack of knowledge of structure-property relationships of organic semiconductors.[1,2] Tackling these challenges, the design and synthesis of organic semiconductors with novel structures, high stability and high mobility are still long-term tasks. Meanwhile, single crystals of organic semiconductors are regarded as one of the best candidates to answer the questions of structure-property relationships of organic semiconductors because of their purity and long range order (free from grain boundaries). Moreover, the high quality of organic crystals could ensure the high performance of organic devices and circuits.[3,4]

Of all organic semiconductors reported so far, pentacene is a benchmark material with the highest mobility.[5] A serious problem of pentacene is that it suffers from the disadvantages of extreme insolubility and instability. It is insoluble in common organic solvents, which limits the advantage of solution processing techniques for device fabrication and self-assembly. Moreover, pentacene degrades rapidly in ambient conditions because of the photo-induced decomposition presumably forming transannular endoperoxide or dimeric Diels–Alder adducts.[1a,6] Therefore, the development of organic semiconductors with pentacene-like structure but better stability is highly attractive, for example, thiophene-based materials (most of which exhibit much better stability compared to pentacene) have recently attracted much attention.[7] An intriguing approach is to combine the high mobility of pentacene and the high stability of thiophene-based materials together to produce fused-ring thienoacenes,[7–13] such as pentathienoacene, tetraceno[2,3-*b*]thiophene, anthradithiophene, and dibenzo[*d*,*d*′]thieno[3,2-*b*;4,5-*b*′]dithiophene *etc.* And these materials indeed showed better stability than that of pentacene together with excellent device performances.

All the reported fused-ring thienoacenes[7–13] have pentacene-like molecular structure, with linear cores and herringbone-like packing motif. However, theoretically, a π-stacking structure is expected to provide more efficient orbital overlap and thereby facilitates carrier transport and gives high mobility.[2] And indeed, some organic semiconductors with close side-by-side π–π stacking give mobilities of thin films as high as 10 $cm^2V^{-1}s^{-1}$.[14] Therefore, it will be highly attractive to design and synthesize fused-ring thienoacenes with a dense π–π molecular packing motif, and to examine the charge transport properties of the compounds to give guidelines for further design and synthesis of high performance organic semiconductors for devices. To our knowledge, no reports have addressed fused-ring thienoacenes with π-stacking structure. Here, we report the first example of a fused-ring thienoacene with sickle-like molecular shape. It has: i) ideal π–π stacking between molecules, ii) excellent solubility in common organic solvents, iii) high stability due to its large optical band gap and low highest occupied molecular orbital (HOMO) energy level, iv) high mobility along the π-stacking direction. It is believed that the compound could act as an ideal system not only to examine the structure-property relationships of fused-ring thienoacenes by tuning of molecular structures, but also to examine molecular interactions of fused-ring thienoacenes for controllable self-assembly.

Results and discussion

Synthesis, UV-vis spectrum and cyclic voltammogram measurements

The synthesis of the sickle-like thienoacene, bis(benzo[4,5]-thieno)[2,3-*b*:3′,2′-*d*]thiophene (BBTT), is shown in Scheme 1. 3-Bromobenzo[*b*]thiophene was treated with 0.5 equivalents of bis(tri-*n*-butyltin) in the presence of $Pd(PPh_3)_4$ to obtain

[a]*Beijing National Laboratory for Molecular Sciences, Key Laboratory of Organic Solids, Institute of Chemistry, Chinese Academy of Sciences, Beijing, P. R. China. E-mail: xwzhan@iccas.ac.cn; huwp@iccas.ac.cn*
[b]*Shanghai Institute of Organic Chemistry, Chinese Academy of Sciences, Shanghai, P. R. China*

† Electronic supplementary information (ESI) available: Optical microscopic images of BBTT ribbons cast assembly on different substrates. CCDC reference number 778225. For ESI and crystallographic data in CIF or other electronic format see DOI: 10.1039/c0jm00963f

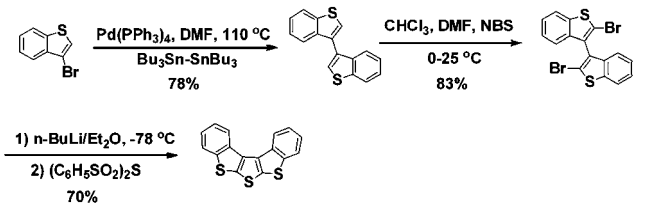

Scheme 1 Synthetic route of BBTT.

3,3′-dibenzothiophene. BBTT was synthesized by bromination of 3,3′-dibenzothiophene, followed by lithiation with *n*-BuLi and cyclization with bis(phenylsulfonyl)sulfide in 58% yield over two steps, somewhat higher than the yields (30–47%) reported by Schroth *et al.*,[15] where treatment of 3,3′-dibenzothiophene with either ethoxycarbonylsulfenyl chloride in the presence of $TiCl_4$ or with *n*-BuLi and then elemental sulfur resulted in the formation of BBTT (see Experimental section for details). BBTT is highly soluble in common organic solvents, suggesting its ideal solubility for solution processes.

UV-vis absorption of BBTT (CH_2Cl_2, $\sim 10^{-5}$ M) is shown in Fig. 1a. The spectrum showed absorption peaks at 253, 308 and 318 nm. The energy gap was estimated at about 3.77 eV from its long absorption edge. This value was around 1.97 eV larger than that of pentacene.[16] The redox behavior of BBTT was examined using cyclic voltammetry (CV) measurements. As shown in Fig. 1b, BBTT showed reversible oxidation waves. The HOMO energy level was determined to be around −5.64 eV from the first oxidation potential with respect to ferrocene (with HOMO level at −4.8 eV), which was 0.57 eV lower than that of pentacene (5.07 eV).[16] The lower HOMO energy level and larger bandgap of BBTT indicate that this compound is hard to be oxidized, *i.e.*, with potential high stability in ambient conditions.

Crystal structure and molecular packing

A needle-like colorless bulk crystal was obtained by slow evaporation of mixed solvent of toluene and trichloromethane (v/v = 1/1) in a closed jar with several pinholes (see ESI for crystallographic data in CIF format†). The X-ray diffraction (XRD) pattern of the crystal suggests it belongs to orthorhombic crystal system, space group $P2_12_12_1$, with $a = 3.8834(8)$ Å, $b = 7.5943(15)$ Å, $c = 41.630(8)$ Å. There are four inequivalent molecules per unit cell and they are symmetrically correlated by a 2_1 screw axis along the *c* axis. A column of molecules stacking down the *a* axis shows the molecular stacking

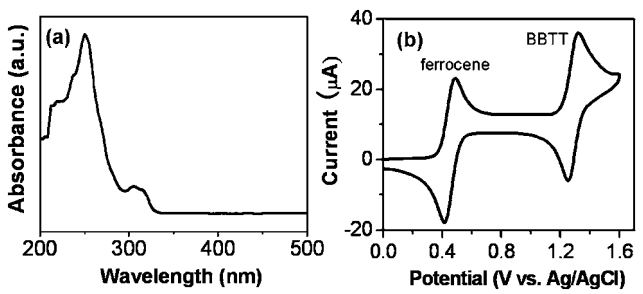

Fig. 1 (a) UV-vis absorption spectrum of BBTT in CH_2Cl_2 ($\sim 10^{-5}$ M), (b) cyclic voltammogram curve of BBTT using Ag/AgCl as reference electrode and ferrocene as internal standard.

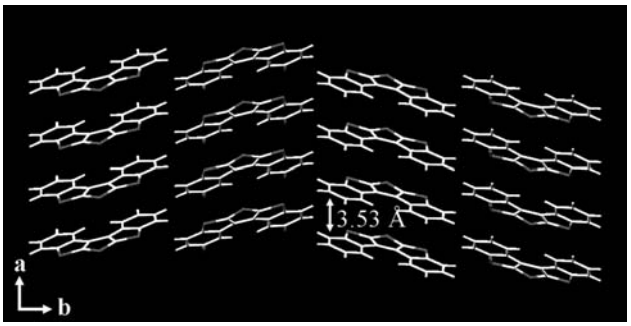

Fig. 2 Crystal packing of BBTT in the *a*-*b* plane with molecular packing distance along the *a* direction at 3.53 Å.

distance at around 3.53 Å (Fig. 2), indicating the strong intermolecular π–π interactions between the stacking molecules. Pitch and roll angles are measured to be 14.43° and 20.32°, respectively. These small angles also demonstrate the good spatial overlap of adjacent molecules and strong intermolecular interactions between the two adjacent molecules along the stacking direction. The close π–π stacking and large spatial overlap of BBTT indicate that strong intermolecular interactions exist in the solid state, which may facilitate the controllable self-assembly to produce micro- and/or nanostructures.

The preliminary self-assembly of BBTT was examined by vacuum deposition of its thin films. Scanning electron microscopy (SEM) images of the films on SiO_2 and OTS (n-octadecyltrichlorosilane) modified SiO_2 substrates are shown in Fig. 3a and b, which appeared as nice rod- or ribbon-like structures instead of homogeneous films, giving direct evidence of strong intermolecular interactions along the long axis of the rods or ribbons.

Self-assembly of BBTT in solution was examined by drop casting. Saturated toluene solution of BBTT was drop-cast on different substrates. Micro- and/or nanometer sized ribbons of BBTT were found to self-assemble efficiently as shown in Fig. 3c and d. The width of the ribbons ranges from tens of nanometers to micrometers with lengths up to hundreds of micrometers. The growth of the ribbons

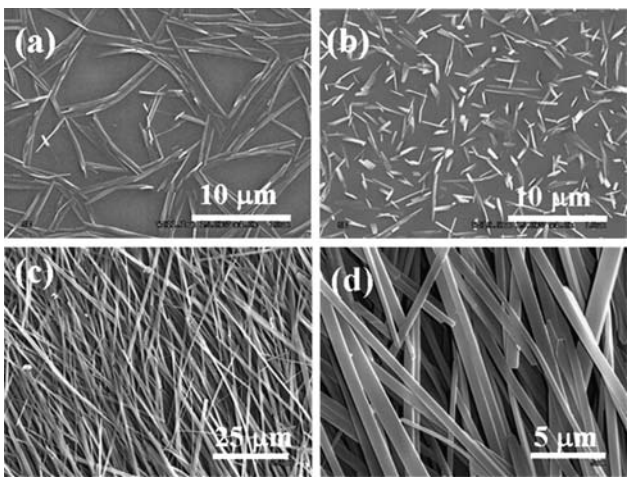

Fig. 3 (a, b) SEM images of vacuum deposited films of BBTT on SiO_2 and OTS modified SiO_2 substrates. (c, d) SEM images of micro- and nanoribbons of BBTT self-assembled by drop casting from saturated toluene solution.

was independent of the substrate as similar ribbons could be obtained on different substrates such as glass, parchment paper, quartz, and plastic (see ESI for optical microscopic images of BBTT ribbons cast assembly on different substrates†). Moreover, the growth of the ribbons was also unaffected by the solvents used (toluene, chlorobenzene, trichloromethane or dichloromethane *etc.*), indicating the weak solvent effect on the self-assembly of micro- and/or nanoribbons of BBTT. Based on the above results, we concluded that it was the internal molecular interactions that drove the formation of the ribbons.

Transmission electron microscopy (TEM) measurements were further used to determine the structure of the ribbons. Saturated toluene solution of BBTT was drop cast on Cu grid (the same method as they were drop cast on OTS/SiO_2/Si wafers). Micro- and/or nanocrystals lying on the carbon film of the Cu grid were obtained by slow evaporation of the solvent. A typical TEM image of an individual ribbon of BBTT is given in Fig. 4a and its corresponding selected area electron diffraction (SAED) pattern is shown in Fig. 4b. No change of the SAED pattern was observed for the different parts of the same crystal, indicating that the whole ribbon was a single crystal. The SAED pattern of the BBTT ribbon was indexed with its crystal lattice constants. It could be concluded that the single crystal ribbon grew along the [101] (or [10$\bar{1}$]) direction, *i.e.*, the π–π interactions along the [101] (or [10$\bar{1}$]) direction resulted in the fastest crystal growth along this direction and thus micro- and/or nanoribbons were obtained.

The XRD pattern of the obtained BBTT ribbons on OTS modified SiO_2 substrates is shown in Fig. 4c. The smooth background and sharp diffraction peaks confirmed the high quality of the crystals. Main reflection peaks are indexed to be (00*l*) with $l = 4$, 8 and 12 according to the single crystal structure. Other reflection peaks are weak compared with the (00*l*) peaks, indicating that (00*l*) planes of the ribbons are parallel to the substrate. Such an orientation is known to be favorable for charge transport in the active layer of organic field-effect transistors (OFETs).

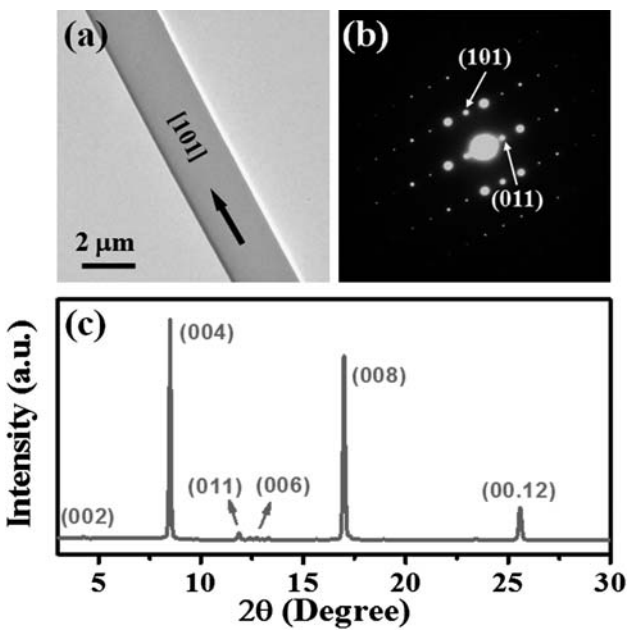

Fig. 4 (a) TEM image and (b) corresponding SAED pattern of an individual ribbon. (c) XRD pattern of the self-assembled single crystalline ribbons of BBTT on OTS modified SiO_2 substrates.

Single-crystal FET characterization

OFETs based on an individual ribbon crystal were fabricated using the "organic ribbon mask" technique,[17] which was performed on a Micromanipulator 6150 probe station with a high resolution microscope (magnification at 400–1000 times). The processes of device fabrication could be divided into 4 steps: i) single crystal ribbons of BBTT were put on OTS/SiO_2/Si substrates by solution casting, ii) an individual ribbon of BBTT (mask ribbon) was picked up by the mechanical probe and laminated crossed over another crystal, iii) Au electrodes (source and drain) were vacuum evaporated on the masked structure, iv) the mask ribbon was peeled off by the mechanical probe. The schematic diagram of the devices fabricated by this technique is shown in Fig. 5a and example optical and SEM images of sample devices are shown in Fig. 5b and c.

Tens of devices have been examined carefully, and the typical output and transfer characteristics of the device are shown in Fig. 5d and e. At the saturation regime of the transfer curve, the current I_{DS} is given by $I_{DS} = (W/2L)\mu C_i(V_G - V_T)^2$, where W is the channel width (here, the width of the ribbon crystal), L is the channel length, and C_i is the capacitance per unit area of the dielectric layer. The mobility of BBTT crystals examined by this technique was around 0.20–0.60 $cm^2 V^{-1} s^{-1}$ with on/off ratios over 10^6. To our knowledge, these parameters are among the top results of organic single crystal transistors from solution processes. And we believe that the performance of the devices of BBTT could be further improved by optimizing the device configurations, *e.g.*, the energy match between the HOMO of BBTT (−5.63 eV) and the Fermi energy of Au electrodes.

Finally, the stability of the single crystal devices was examined by two series of measurements: the stability under continuous operation conditions and long-term stability (stored in air over 3 months). It was found that during the 30-cycle continuous voltage sweep, most devices showed no observable degradation in performance (mobility and on/off ratio). The long-term stability of the devices was examined

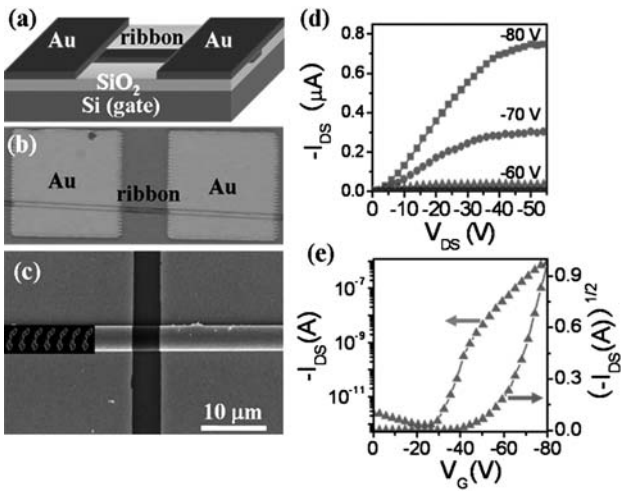

Fig. 5 (a) Schematic diagram and (b, c) optical and SEM images of example OFETs based on individual BBTT single crystal ribbons, (d, e) typical output and transfer characteristics of the devices (here channel length $L = 4.9$ μm, channel width $W = 5.4$ μm).

over 3 months. The mobility and on/off ratio had some decrease in the first few days and reached a stable point with little degradation. Furthermore, even after storing over 3 months in air, the devices were still stable under continuous operation conditions. These results definitely confirmed the good stability of BBTT OFETs under continuous operation conditions and long-term storage conditions in air, which could be attributed to the high stability of BBTT.

Conclusions

In summary, the solution self-assembly and charge transport properties of BBTT, a fused-ring thienoacene with sickle-like molecular shape, were studied. BBTT adopted a π–π stacking structure in the single crystal, which was distinctly different from the linear fused-ring thienoacenes with a herringbone packing motif. Strong intermolecular interactions in BBTT drove the efficient self-assembly of one-dimensional single crystalline ribbons by drop casting irrespective of the substrates and solvents used. OFETs based on an individual ribbon were examined, which exhibited not only high mobility (up to 0.6 $cm^2\ V^{-1}\ s^{-1}$), but also high stability. The strong π–π stacking structure, excellent solubility, high mobility and good stability as well as the facile assembly ability of BBTT give useful clues for further design of high performance materials and indicate its great application potential in organic electronics.

Experimental

Measurements

UV-vis spectra were recorded using a Hitachi U-3010 spectrometer. CV was run on a CHI660C electrochemistry station using tetrabutylammonium hexafluorophosphate (Bu_4NPF_6, 0.1 mol/L) as electrolyte with glassy carbon as a working electrode, Pt wire as a counter electrode, and Ag/AgCl as a reference electrode. SEM images were obtained on a Hitachi S-4300 SEM (Japan). TEM samples were prepared by drop casting of a saturated toluene solution of BBTT on a Cu grid. TEM observation and SAED were carried out on a JOEL 2011. The current–voltage (*I–V*) characteristics were measured with a Micromanipulator 6150 probe station in a clean and metallic shielded box at room temperature in air, and recorded with a Keithley 4200 SCS.

Synthesis of BBTT

[3,3′]Bi[benzo[*b*]thiophenyl]. To a 100 mL round-bottom flask were added 3-bromobenzothiophene (10 mmol, 2.13 g), bis-(tributyltin) (5 mmol, 2.9 g), and dry DMF (20 mL); the mixture was deoxygenated with nitrogen for 30 min. $Pd(PPh_3)_4$ (0.20 mmol, 232 mg) was added under nitrogen. The mixture was stirred at 110 °C for 48 h. After cooling to room temperature, the mixture was washed with 10 mL aqueous KF (1.5 g), then extracted with methylene chloride (2 × 100 mL). The organic layer was washed with water (2 × 300 mL), and dried over anhydrous $MgSO_4$. After removal of solvent, the residue was purified by column chromatography on silica gel using hexanes as eluent to afford 3,3′-dibenzothiophene as a white solid (1.04 g, 78%). ^{1}H NMR (400 MHz, $CDCl_3$): δ 7.99 (dd, J = 7.0, 1.2 Hz, 2H), 7.79 (dd, J = 7.0, 1.2 Hz, 2H), 7.55 (s, 2H), 7.46–7.34 (m, 4H). ^{13}C NMR (100 MHz, $CDCl_3$): δ 140.15, 138.52, 131.35, 124.70, 124.58, 124.28, 123.19, 122.80. MS (EI): 266 (M^+).

2,2′-Dibromo-[3,3′]bi[benzo[*b*]thiophenyl]. A mixture of [3,3′]bi[benzo[*b*]thiophenyl] (5.64 mmol, 1.5 g) and chloroform (20 mL) in a 100 mL round-bottom flask wrapped with aluminium foil was cooled to 0 °C. NBS (11.2 mmol, 1.99 g) in DMF (20 mL) was added dropwise over a period of 5 min. The mixture was stirred at 0 °C for 1 h, then warmed to room temperature and stirred for 4 h. The mixture was poured into ice-cold 2 M aqueous NaOH (200 mL), and stirred for 10 min. The product was extracted with dichloromethane (100 mL × 2); the organic layer was washed with water (200 mL × 2), and dried over anhydrous $MgSO_4$. After removing the solvent, the residue was purified by column chromatography on silica gel using hexanes as eluent and recrystallization from hexanes yielding white crystals (1.98 g, 83%). ^{1}H NMR (400 MHz, $CDCl_3$): δ 7.80 (d, J = 8.1 Hz, 2H), 7.34 (m, 2H), 7.26 (m, 4H). ^{13}C NMR (100 MHz, $CDCl_3$): δ 139.80, 138.09, 130.05, 124.98, 124.89, 122.96, 121.82, 116.89. MS (EI): 424 (M^+). Anal Calcd. for $C_{16}H_8Br_2S_2$: C, 45.30; H, 1.90. Found: C, 45.21; H, 1.86%.

***syn*-Bis(benzothieno)thiophene.** 2.5 M *n*-BuLi in hexane (9 mmol, 3.6 mL) was added dropwise over 10 min under nitrogen to a magnetically stirred solution of 2,2′-dibromo-[3,3′]bi[benzo[*b*]thiophenyl] (4 mmol, 1.7 g) in anhydrous THF (40 mL) which was maintained at −78 °C by means of a dry ice–acetone cooling bath. The solution was kept at −78 °C with stirring for 1 h. Then bis(phenylsulfonyl)sulfide (4 mmol, 1.3 g) was added portionwise. Stirring was continued at −78 °C for 2 h, then the mixture was allowed to gradually warm to room temperature, and stirred at this temperature overnight. The mixture was washed with water (200 mL), extracted with diethyl ether (2 × 150 mL), and the extracts were dried over anhydrous $MgSO_4$ before being evaporated to dryness. The residue was purified by flash column chromatography (silica gel, using hexane as eluent) and recrystallization from ethanol/benzene (2 v/v) to afford white crystals (0.83 g, 70%). ^{1}H NMR (400 MHz, $CDCl_3$): δ 8.57 (d, J = 8.1 Hz, 2H), 7.87 (d, J = 8.1 Hz, 2H), 7.53 (t, J = 8.1 Hz, 2H), 7.38 (t, J = 8.1 Hz, 2H). ^{13}C NMR (100 MHz, $CDCl_3$): δ 143.08, 139.50, 134.48, 132.44, 124.63, 123.88, 123.40, 123.11. HRMS (EI): 295.9774 (calcd for $C_{16}H_8S_3$: 295.9788). Anal Calcd. for $C_{16}H_8S_3$: C, 64.83; H, 2.72. Found: C, 64.91; H, 2.86%.

Acknowledgements

The authors are grateful to Prof. Zhaohui Wang (Institute of Chemistry) for profound discussion, the financial support from National Natural Science Foundation of China (20721061, 20872146, 50725311), TRR61 (NSFC-DFG Transregio project), Ministry of Science and Technology of China (2006CB806200, 2006CB932100) and Chinese Academy of Sciences.

Notes and references

1 (*a*) H. Klauk, *Organic Electronics Materials, Manufacturing and Applications*, Wiley-VCH, Weinheim, 2006; (*b*) Z. Bao and J. Locklin, *Organic Field-Effect Transistors*, Taylor & Francis Group, Boca Raton, 2006; (*c*) W. Brutting, *Physics of Organic Semiconductors*, Wiley-VCH, Weinheim, 2005.

2 (*a*) J. L. Brédas, D. Beljonne, V. Coropceanu and J. Cornil, *Chem. Rev.*, 2004, **104**, 4971; (*b*) C. Reese and Z. Bao, *J. Mater. Chem.*, 2006, **16**, 329; (*c*) V. Coropceanu, J. Cornil, D. A. da Silva Filho, Y. Olivier, R. Silbey and J. L. Brédas, *Chem. Rev.*, 2007, **107**, 926.

3 (*a*) R. Li, W. Hu, Y. Liu and D. Zhu, *Acc. Chem. Res.*, 2010, **43**, 529; (*b*) L. Jiang, H. Dong and W. Hu, *J. Mater. Chem.*, 2010, **20**, DOI: 10.1039/b925875b; (*c*) S. Liu, W. M. Wang, A. L. Briseno, S. C. B. Mannsfeld and Z. Bao, *Adv. Mater.*, 2009, **21**, 1217; (*d*) C. Reese and Z. Bao, *Mater. Today*, 2007, **10**, 20; (*e*) M. E. Gershenson, V. Podzorov and A. F. Morpurgo, *Rev. Mod. Phys.*, 2006, **78**, 973; (*f*) R. W. I. de Boer, M. E. Gershenson, A. F. Morpurgo and V. Podzorov, *Phys. Status Solidi A*, 2004, **201**, 1302.

4 (*a*) C. Kloc, K. J. Tan, M. L. Toh, K. K. Zhang and Y. P. Xu, *Appl. Phys. A: Mater. Sci. Process.*, 2009, **95**, 219; (*b*) A. S. Molinari, H. Alves, Z. Chen, A. Facchetti and A. F. Morpurgo, *J. Am. Chem. Soc.*, 2009, **131**, 2462; (*c*) Q. Tang, Y. Tong, W. Hu, Q. Wan and T. Bjørnholm, *Adv. Mater.*, 2009, **21**, 4234; (*d*) R. Li, H. Li, Y. Song, Q. Tang, Y. Liu, W. Xu, W. Hu and D. Zhu, *Adv. Mater.*, 2009, **21**, 1605; (*e*) L. Jiang, W. Hu, Z. Wei, W. Xu and H. Meng, *Adv. Mater.*, 2009, **21**, 3649; (*f*) A. L. Briseno, S. C. B. Mannsfeld, M. M. Ling, S. Liu, R. J. Tseng, C. Reese, M. E. Roberts, Y. Yang, F. Wudl and Z. Bao, *Nature*, 2006, **444**, 913; (*g*) V. C. Sundar, J. Zaumseil, V. Podzorov, E. Menard, R. L. Willett, T. Someya, M. E. Gershenson and J. A. Rogers, *Science*, 2004, **303**, 1644; (*h*) V. Podzorov, V. M. Pudalov and M. E. Gershenson, *Appl. Phys. Lett.*, 2003, **82**, 1739; (*i*) R. W. I. de Boer, T. M. Klapwijk and A. F. Morpurgo, *Appl. Phys. Lett.*, 2003, **83**, 4345.

5 (*a*) D. J. Gundlach, Y.-Y. Lin, T. N. Jackson, S. F. Nelson and D. G. Schlom, *IEEE Electron Device Lett.*, 1997, **18**, 87; (*b*) Y.-Y. Lin, D. J. Gundlach, S. F. Nelson and T. N. Jackson, *IEEE Electron Device Lett.*, 1997, **18**, 606.

6 A. Maliakal, K. Raghavachari, H. Katz, E. Chandross and T. Siegrist, *Chem. Mater.*, 2004, **16**, 4980.

7 (*a*) M. L. Tang, S. C. B. Mannsfeld, Y. S. Sun, H. A. Becerril and Z. Bao, *J. Am. Chem. Soc.*, 2009, **131**, 882; (*b*) M. Tang, A. Reichardt, N. Miyaki, R. M. Stoltenberg and Z. Bao, *J. Am. Chem. Soc.*, 2008, **130**, 6064; (*c*) T. Okamoto, M. L. Senatore, M.-M. Ling, A. B. Mallik, M. L. Tang and Z. Bao, *Adv. Mater.*, 2007, **19**, 3381; (*d*) J. Roncali, *Chem. Rev.*, 1992, **92**, 711.

8 (*a*) K. Xiao, Y. Liu, T. Qi, W. Zhang, F. Wang, J. Gao, W. Qiu, Y. Ma, G. Cui, S. Chen, X. Zhan, G. Yu, J. Qin, W. Hu and D. Zhu, *J. Am. Chem. Soc.*, 2005, **127**, 13281; (*b*) X. Zhang, A. P. Cote and A. J. Matzger, *J. Am. Chem. Soc.*, 2005, **127**, 10502; (*c*) M. Yasuhiro and K. Keiji, *Tetrahedron Lett.*, 1989, **30**, 3315.

9 M. L. Tang, T. Okamoto and Z. Bao, *J. Am. Chem. Soc.*, 2006, **128**, 16002.

10 J. G. Laquindanum, H. E. Katz and A. J. Lovinger, *J. Am. Chem. Soc.*, 1998, **120**, 664.

11 (*a*) A. R. Murphy and J. M. J. Fréchet, *Chem. Rev.*, 2007, **107**, 1066; (*b*) R. A. Pascal Jr., *Chem. Rev.*, 2006, **106**, 4809; (*c*) J. E. Anthony, *Chem. Rev.*, 2006, **106**, 5028.

12 (*a*) J. Wang, Y. Zhou, J. Yan, L. Ding, Y. Ma, Y. Cao, J. Wang and J. Pei, *Chem. Mater.*, 2009, **21**, 2595; (*b*) J. E. Anthony, *Angew. Chem., Int. Ed.*, 2008, **47**, 452; (*c*) H. Okamoto, N. Kawasaki, Y. Kaji, Y. Kubozono, A. Fujiwara and M. Yamaji, *J. Am. Chem. Soc.*, 2008, **130**, 10470; (*d*) C. Du, Y. Guo, Y. Liu, W. Qiu, H. Zhang, X. Gao, Y. Liu, T. Qi, K. Lu and G. Yu, *Chem. Mater.*, 2008, **20**, 4188; (*e*) Y. Zhou, W. Liu, Y. Ma, H. Wang, L. Qi, Y. Cao, J. Wang and J. Pei, *J. Am. Chem. Soc.*, 2007, **129**, 12386; (*f*) M. Kuo, H. Chen and I. Chao, *Chem.–Eur. J.*, 2007, **13**, 4750; (*g*) F. Valiyev, W. Hu, H. Chen, M. Kuo, I. Chao and Y. Tao, *Chem. Mater.*, 2007, **19**, 3018.

13 (*a*) J. Gao, R. Li, L. Li, Q. Meng, H. Jiang, H. Li and W. Hu, *Adv. Mater.*, 2007, **19**, 3008; (*b*) R. Li, L. Jiang, Q. Meng, J. Gao, H. Li, Q. Tang, M. He, W. Hu, Y. Liu and D. Zhu, *Adv. Mater.*, 2009, **21**, 4492.

14 (*a*) Y. Takahashi, T. Hasegawa, S. Horiuchi, R. Kumai, Y. Tokura and G. Saito, *Chem. Mater.*, 2007, **19**, 6382; (*b*) L. Li, Q. Tang, H. Li, X. Yang, W. Hu, Y. Song, Z. Shuai, W. Xu, Y. Liu and D. Zhu, *Adv. Mater.*, 2007, **19**, 2613.

15 W. Schroth, E. Hintzsche, H. Jordan, T. Jende, R. Spitzner and I. Thondorf, *Tetrahedron*, 1997, **53**, 7509.

16 T. Yasuda, T. Goto, K. Fujita and T. Tsutsui, *Appl. Phys. Lett.*, 2004, **85**, 2098.

17 L. Jiang, J. Gao, E. Wang, H. Li, Z. Wang, W. Hu and L. Jiang, *Adv. Mater.*, 2008, **20**, 2735.

